# Shift in electrocorticography electrode locations after surgical implantation in children

A thesis submitted to the University of Arizona College of Medicine – Phoenix
in partial fulfillment of the requirements for the Degree of Doctor of Medicine

Bryce Munter
Class of 2021

Mentor: Stephen T. Foldes, PhD

# Shift in electrocorticography electrode locations after surgical implantation in children

Bryce T Munter, MSE, Stephen T Foldes, PhD, Brian L Appavu, MD, John F Kerrigan, MD, P. David Adelson, MD

## Highlights

• The brain shifts in response to ECoG implantation surgery which can impact the spatial interpretation of electrode locations.

• The amount of shift in ECoG electrode locations immediately after implant in a pediatric population was 5.64 ± 3.27 mm.

• This shift was significantly greater with larger estimated intracranial volume, in the parietal lobe, and on grids compared to strips.

• The shift in ECoG immediately after implantation could lead to a misinterpretation of contact location particularly in patients with larger intracranial volume and for grid contacts over the parietal lobes.

## Abstract

Interpreting electrocorticography (ECoG) in the context of neuroimaging requires that multimodal information be integrated accurately. However, the implantation of ECoG electrodes can shift the brain impacting the spatial interpretation of electrode locations in the context of pre-implant imaging. We characterized the amount of shift in ECoG electrode locations immediately after implant in a pediatric population. Electrode-shift was quantified as the difference in the electrode locations immediately after surgery (via post-operation CT) compared to the brain surface before the operation (pre-implant T1 MRI). A total of 1140 ECoG contracts were assessed across 18 patients ranging from 3 to 19 (12.1 ± 4.8) years of age who underwent intracranial monitoring in preparation for epilepsy resection surgery. Patients had an average of 63 channels

assessed with an average of 5.64 ± 3.27 mm shift from the pre-implant brain surface within 24 h of implant. This shift significantly increased with estimated intracranial volume, but not age. Shift also varied significantly depending of the lobe the contact was over; where contacts on the temporal and frontal lobe had less shift than the parietal. Furthermore, contacts on strips had significantly less shift than those on grids. The shift in the brain surface due to ECoG implantation could lead to a misinterpretation of contact location particularly in patients with larger intracranial volume and for grid contacts over the parietal lobes.

## Abbreviations

ECoG - electrocorticography
eTIV - estimated total intracranial volume
DBS - deep brain stimulation
RNS - responsive neurostimulation
SCE - smoothed cortical envelope

## Keywords

Electrocorticography
Surgery
Pediatric

## 1. Introduction

Recording electrical activity directly from the brain surface with subdural electrocorticography (ECoG) has tremendous value in epilepsy surgical, neuroscience, and developing neurotechnology. As the imaging and electrophysiology methods for diagnosing epilepsy advance, there is a need for combining information across data types by localizing intracranial electrodes on imaging data (Bayer et al., 2017). For example, mapping ictal electrographic activity could be enhanced by overlapping cortical thickness information derived from MRI in cases of focal cortical dysplasia (Adler et al., 2017). To take advantage of multimodal information, the relative locations of the ECoG electrodes to the brain anatomy need to be known. However,

co-localizing post-implant electrode locations on pre-implant imaging data can be challenging (Bayer et al., 2017; Nimsky et al., 2000). A key challenge for localization is accounting for brain shift, where the operative placement of the electrodes leads to temporary deformation of the tissue.

Brain shift is a deformation of tissue that occurs after a brain surgery due to several factors including brain retraction, cerebral edema, excision of tissue, drainage of cerebrospinal fluid, and surgical intervention. Average post-surgical brain shifts has been reported between 3 and 24 mm (Elias et al., 2007; Hastreiter et al., 2004; Hill et al., 1998; Hinds et al., 2018; Letteboer et al., 2005; Nimsky et al., 2000; Roberts et al., 1998; Van Rooijen et al., 2013; Yang et al., 2017). In adults, the amount of shift from different types of surgeries has been shown to be independent of sex, age, craniotomy size, preoperative ventricular volume, surgery duration, and preoperative diagnosis (Elias et al., 2007; Letteboer et al., 2005; Roberts et al., 1998; Yang et al., 2017) in adults. Unsurprisingly, brain shift was found to significantly correlate with volume of pneumocephalus (an approximation of CSF loss), durotomy size, and resection size (Elias et al., 2007; Yang et al., 2017). The need to account for brain shift has been identified in pediatric populations and imaging analysis methods have been explored (Beare et al., 2016; Ducis et al., 2016; Taimouri et al., 2014; Yang et al., 2017), but no work has characterized this shift at the cortical surface in children.

The discrepancy in ECoG electrode location due to brain shift at the cortical surface can impact the interpretation of electrophysiological data and compromise clinical accuracy of neuronavigation systems (Bayer et al., 2017; Ducis et al., 2016; Nimsky et al., 2000). The amount of shift and its potential impact in interpreting ECoG information are unknown in pediatric populations. In this study, we quantify the post-implant shift in ECoG contact location for pediatric patients. Our primary aims are to determine if the shift is dependent on estimated total intracranial volume (eTIV), age, or brain cortical region directly underneath the electrode.

# 2. Methods

### 2.1. Patients

This was a retrospective analysis of patients who underwent intra-cranial monitoring with surface ECoG in preparation for resective epilepsy surgery at Phoenix Children's

Hospital (IRB: #17-052). All patients were diagnosed with drug resistant localization related epilepsy. All surgeries were performed at Phoenix Children's Hospital by the same surgeon (PDA) from 2014 to 2018. A total of 18 patients ranging from 3 to 19 (12.1 ± 4.8) years old at time of surgery with 11 males, 7 females were analyzed. (Table 1). Three other patients were identified but not included in the study due to MRI artifacts from VNS (n = 1) and large previous resections (n = 2).

Table 1. Demographics and surgery information.

| **SEX** | **n** |
|---|---|
| **Female** | 7 (39 %) |
| **Male** | 11 (61 %) |
| **PATHOLOGY** | n |
| **Cortical dysplasia** | 10 (56 %) |
| **Normal parenchyma** | 4 (22 %) |
| **Tumor(s)** | 2 (11 %) |
| **Neurofibromatosis** | 1 (6 %) |
| **Tuberous Sclerosis** | 1 (6 %) |

All patients underwent a craniotomy for placement of brain surface ECoG electrodes that were configured in a grid (8 × 8, 64 contact grid) or strip (1 × 6 or 1 × 8 configuration) (PMT Corporation, Chanhassen, MN, USA). Contacts were platinum–iridium alloy electrode disks (4 mm dia.) with inter-electrode spacing of 10 mm. Grids were sutured to the edges of the dura to prevent movement. After implantation and tunneling of the wires, each of the electrodes were secured individually in 2 locations by suturing them to the dura and at the exit sites at the skin. The dura was closed in a tension-free way using an allograft patch using non-synthetic dura substitute (Durarepair). The bone was replaced rigidly, fixed with mini-plates and screws. No drain was used for brain relaxation, though Mannitol (0.25 g per kg) was given every 6 h for 48 h. Some depth/ intraparenchymal EEG wires were placed in addition to surface ECoG. However, depth electrodes are not expected to have substantial shift (Dalal et al., 2008; Ivan et al., 2014; Yang et al., 2012) and could not be assessed using the brain-surface analysis presented here and were therefore not assessed.

### 2.2. Imaging

Pre-implant 3D T1 MRI images were acquired on a Philips 3 T scanner and incorporated into standard pre-surgical planning. The pre-implant MRI was segmented using Freesurfer software (version 6.0) (Fischl, 2012) to generate 3D models of the pial surface. A 3D mesh surface of the outside of the cortex for each hemisphere was created (via local gyrification index function (Schaer et al., 2008)). This smoothed cortical envelope (SCE) of the brain was used to account for the electrodes sitting above sulci (Blenkmann et al., 2017).
CT scan of the head using bone windows with 3D reconstructions were acquired on a Phillips Brilliance iCT scanner within 24 h but most often on transport from the operating room en route to the ICU after implantation of the intracranial EEG electrodes. CTs were captured at 0.46 × 0.46 × 1 mm and MRIs at 0.51 × 0.51 × 0.9 mm. Patients were supine for both MRI and CT imaging. The pre-implant T1 MRI and post-operative CT showing ECoG locations were then co-registered with a rigid body transformation via SPM12 (Wellcome Trust Centre for Neuroimaging, UCL) (Hinds et al., 2018; Penny et al., 2007). This methodology for image co-registration between pre- and post- surgery has been validated in children (Beare et al., 2016). Co-registration fit was inspected for all cases. The location of the electrodes on the co-registered-CT images were manually marked based on cluster analysis of the high intensity values of the metal contacts in the CT using iElectrodes software (Blenkmann et al., 2017).

### 2.3. Calculating shift

Shift in electrode location was quantified as the distance between the electrode locations on the co-registered post-implant CT compared to the pre-implant smoothed brain surface (i.e. the SCE computed from the MRI). A simple projection of each contact to the closest point on the SCE would not have taken into consideration the physical rigidity of the grid/strip configurations (e.g. contact spacing would not be explicitly maintained during the projection). Instead, electrodes were projected to the SCE using an algorithm that accounted for the displacement of the electrodes while minimizing the deformation of the connections between contacts (Dykstra et al., 2012). This method has been well validated elsewhere, and the algorithm has demonstrated accuracy to a 0.2mm resolution (Blenkmann et al., 2017; Branco et al.,

2018; Hermes et al., 2010; Stolk et al., 2018). The specific implementation of this algorithm was part of the iElectrodes toolbox (Blenkmann et al., 2017). Individual electrodes were removed from the analysis if their location was over an area where the SCE could not be well computed, e.g. a previous resection.
Compression and shear components of the shift were determined for a secondary analysis of the electrode offsets. The compression-offset was defined as movement out from the center of the brain (i.e. the radial component of the projection-vector). The shear-offset was determined as the component tangential to the compression-offset.

### 2.4. Statistics

The amount of shift at each contact was considered in the context of patient age at surgery, eTIV, lobe under the contact, and if the contact was part of a grid or strip using a mixed effects model. Additional fixed effects were the days between the pre-surgical T1 and post-surgical CT and the interaction of age and eTIV. Patient id was included as a random effect. eTIV was calculated using FreeSurfer (Buckner et al., 2004). Electrodes were manually categorized by lobe.

## 3. Results

### 3.1. Electrode shift

A total of 1140 ECoG contacts were assessed across 18 patients. Patients' eTIV ranged from 893 to 2244 $cm^3$ (1404 ± 322). A total of 43 out of 1183 contacts were removed from the analysis based on their location over small resections/lesions, crossing hemispheres, or interhemispheric placement. No cases of brain hemorrhage were found in the post-implant CTs. The number of valid electrodes per patient ranged from 24 to 83 (63.3 ± 16.7). Electrodes shift ranged from 0.0 to 17.0 mm with an average of 5.6 ± 3.3 mm shift from the original brain surface immediately after implant (Fig. 1).

Shift was significantly affected by eTIV ($p = 0.038$, mixed model), lobe ($p < 0.001$), and grid/strip ($p < 0.001$), but not age ($p = 0.926$). Fig. 2 shows this relationship

between shift and volume (left) and age (right). Age and eTIV were not significantly related (linear regression analysis, $R^2 = 0.14$, $p = 0.132$). Fig. 1 shows this relationship between age and volume. Contacts in grids had significantly more shift than those of the strips ($p < 0.001$) (see Fig. 3). Multi-comparisons analysis by lobe found parietal contacts were significantly more shifted than frontal and temporal contacts ($p < 0.001$ Tukey) (Fig. 3). There were no contacts over the occipital lobe in this cohort.

The majority of the electrode offset was due to movement in the direction out of the brain (i.e. the direction of "compression"). The amount of compression-shift (median ± IQR: 4.9 ± 4.9 mm) was significantly greater than shear (median ± IQR: 1.8 ± 2.0 mm) (Wilcoxon Sign Rank, $p < 0.001$) (Fig. 4). For 95 % of electrodes the shift was comprised of ≥ 92.6 % compression. The same statistical relationships were found when only considering compression as the total-shift, but not when considering shear.

## 4. Discussion

As expected, ECoG contacts were offset relative to pre-implant imaging. In this cohort, the location of the ECoG contacts immediately after implant were shifted by an average of > 5 mm. This shift was just over half the distance between the electrodes (10 mm), but is relatively small considering typical resection sizes. However, this offset still needs to be considered as part of the decision-making process when discussing the potential extent of resection and in the context of minimally invasive surgeries.

Though most previous studies are focused on the surgical impact of brain shift, most have reported similar amounts of brain shift. Brain shift was measured at 5.6 ± 1.9 mm 1 h into adult craniotomy procedures just prior to tumor resection (Hill et al., 1998). Hinds et al. measured 5.4 ± 3.8 mm of ECoG contact offset between pre-implant MRI and immediate post-implant CT in 30 adults using related co-registration methods to ours (Hinds et al., 2018). LaViolette et al. found in 10 adults that ECoG contact positions move 5.4 ± 1.6 mm over 2.9 days from the time of initial implant until after the reopening (LaViolette et al., 2011). Though this is not the time period our study evaluated, this is further evidence that a 5 mm discrepancy should be

considered when relating ECoG contact locations to imaging data. Other brain structures have also been assessed for shift. Letteboer et al. used ultrasound just after opening the dura of adults and found an average parallel shift of other dura areas of 3.0 mm and perpendicular shift of 3.9 mm, though they did not inspect the cortex shift directly (Letteboer et al., 2005). Yang et al. evaluated the shift of white matter tracts during epilepsy resection surgery in 16 children and found an average white matter shift in the operative hemisphere of 2.19 mm (Yang et al., 2017). However, they did not evaluate the shift of the brain surface or the impact of placing ECoG.

Our study is the first to demonstrate that the displacement of electrode contacts after surgery is dependent on intracranial volume (i.e. eTIV). Of further interest, the shift was not dependent on age. In our cohort, age was not correlated with intracranial volume as one might initially expect. This lack of correlation between intracranial volume and age is likely due to the variability in head size in children and specifically in patients undergoing epilepsy surgery. Interestingly, the intracranial volume of our cohort was near that of healthy adults (1404 ± 322 vs. 1469.1 ± 155.79 for 63 healthy adults 26–55 yo (Buckner et al., 2004)), suggesting that the relationship between shift and eTIV is not specific to a pediatric population and these results may apply to all age groups. The dependence of shift on intracranial volume makes sense in the context of the mechanism that cerebral spinal fluid loss during implant surgery and the placement of intracranial hardware causes shift and that individuals with larger intracranial volumes would lose more CSF than those with smaller volumes.

Studies of brain shift from DBS implant for movement disorders have evaluated shift across the brain and have found significant shift specifically in the frontal lobe. Elias et al. reported frontal cortex shift average of 3.51 ± 2.02 mm with a maximum surface shift of 10.9 mm (Elias et al., 2007). Ivan et al. found minimal overall shift due to the DBS burr hole to be 0.7 mm on average, but the frontal lobe had the greatest shift of 1.4 mm on average and a maximum of 10.1 mm ipsilateral to the burr hole procedure (Ivan et al., 2014). Surface shift occurs throughout surgery and during recovery, and is attributable to mechanical tissue properties, loss of CSF, anatomical constraints, tissue resection and removal, intracranial pressure, time after surgery, and, most importantly, gravity (Nabavi et al., 2001; Škrinjar et al., 2002). We observed that electrodes placed in the temporal and frontal lobe shifted less than those in more superior areas (i.e. parietal). This is consistent with previous findings that show shift occurs less on the

inferior surfaces due to the pressure caused by gravity when the patient is sitting (Nabavi et al., 2001).
We also found that ECoG strips had significantly less shift than grids. The strips were inserted to supplement a grid and were placed on the brain surface beyond the edges of the craniotomy to monitor the inferior temporal lobe or the orbital frontal cortex. As expected from their placement, gravity prevented greater shifting. Considering that short ECoG strips are often used for current responsive neurostimulation (RNS) systems, the shift of 3.10 ± 2.27 mm we found across 111 strip contacts may represent the shift occurring for RNS.

The temporal dynamics of shift recovery are not well characterized, but it has been estimated that it takes 3–14 days in adults undergoing DBS implant (Sillay et al., 2013). We evaluated the electrode shift at a single time point, <24 h post-implant, because this is 1) when localization data are available in a typical clinical environment and 2) around the earliest time when iEEG are interpreted. Further movement of the electrodes is expected during the patient's monitoring visit and again during a resection surgery (LaViolette et al., 2011). This further movement of the contacts after the post-implant CT could provide additional challenges in interpreting contact locations on pre-implant imaging, especially when considering the impact of the surgery to reopen the brain for resection. However, this study does not aim to address this. This study also cannot speak to the cause of the electrode shift. It is possible that forces were applied to the electrodes or brain between the time of implant and CT that were unrelated to surgery and account for some of the shift. This was not expected since there were no events reported that could account for external sources of electrode movements before the CT (e.g. reopening, trauma, or electrode lead manipulations). Instead, the goal of this study was to quantify the offset in subdural electrode locations seen by the epileptologists as they read the EEG during typical clinical procedures, regardless of the cause. Therefore, this ∼5 mm shift could be considered the minimum discrepancy between contact location and pre-implant brain surface.
Accounting for this shift may be of immediate importance when considering advanced signal processing methods of iEEG that require intensive analysis and are therefore limited to selected time. For example, 10 min to 2 h of high-frequency oscillations are

typically evaluated during only the first evening after implantation (Cimbalnik et al., 2018; Gliske et al., 2018; Jacobs et al., 2018). From our cohort, the location of these data would be misinterpreted by >5 mm on average.

This brain surface shift is relatively minimal compared to typical resection margins, however, surgeries are becoming less invasive with use of laser interstitial thermal therapy (Wu et al., 2019), high frequency ultrasound, etc. and more targeted with neural stimulation (e.g. responsive neurostimulation) leading to a need for submillimeter localization and interpretation may require a re-assessment to ensure accuracy. Also, as imaging and electrophysiologic methods are improved, clinicians need to be aware of potential limitations of interpretation from the techniques they utilize.

## Acknowledgements

The authors would like to express gratitude to Zachary Humphreys, Austin Jacobson, Ladan Kamali Sarvestani, and Aaron Raber for assistance in method development and data analysis. This work was supported by the Phoenix Children's Hospital Foundation Leadership Circle Award, NSF I/UCRCBuilding Reliable Innovation and Advances in Neurotechnology (Award #1650566), and Phoenix Children's Hospital Innovators in Neuroscience for Kids Foundation. Its contents are the responsibility of the authors and do not necessarily represent the view of the funding agencies.

## Figures

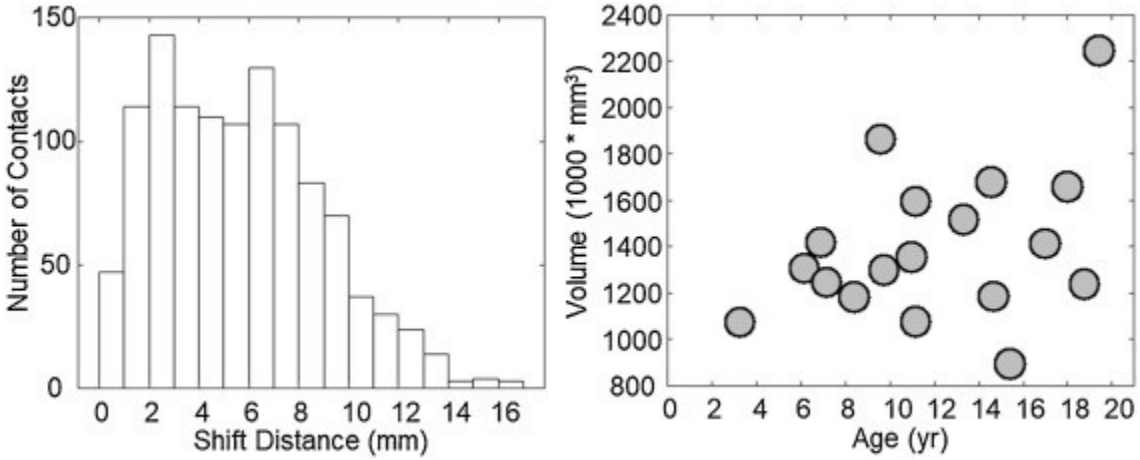

Fig. 1. Distribution of ECoG location shift distances across contacts (Left) and relationship of age to eTIV (Right). Age and eTIV were not significantly related in this cohort.

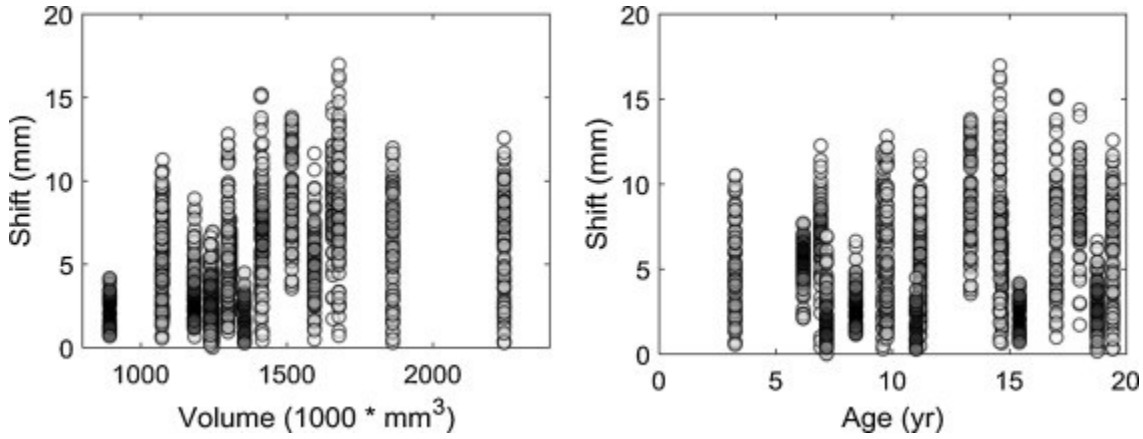


Fig. 2. ECoG location shift at each contact compared to age (A) and eTIV (B). Shift was significantly affected by eTIV but not age.

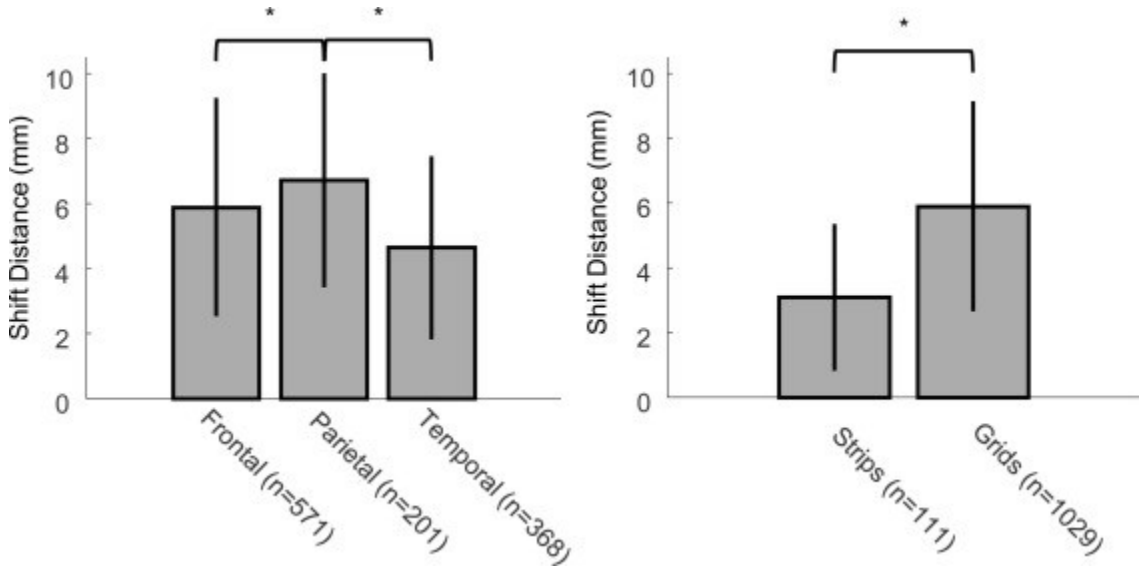


Fig. 3. Shift distance by lobe and strip/grid categorization. Significantly greater shift occurred in the Parietal lobe and in grids. Bars represent the mean and error bars are standard deviation.

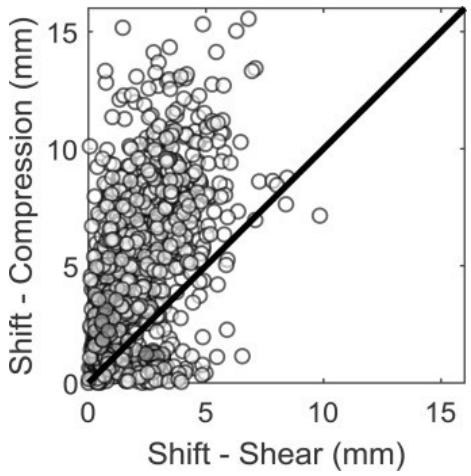


Fig. 4. The relationship between compression and shear components of the electrode shift. There was significantly greater compression than shear. ≥ 92.6 % of the electrode shift was explained by the compression component for 95 % of electrodes.

# References


S. Adler, K. Wagstyl, R. Gunny, L. Ronan, D. Carmichael, J.H. Cross, P.C. Fletcher, T. Baldeweg**Novel surface features for automated detection of focal cortical dysplasias in paediatric epilepsy**

Neuroimage Clin., 14 (2017), pp. 18-27,

S. Bayer, A. Maier, M. Ostermeier, R. Fahrig**Intraoperative imaging modalities and compensation for brain shift in tumor resection surgery**
Int. J. Biomed. Imaging (2017),

R. Beare, J.Y.M. Yang, W.J. Maixner, A.S. Harvey, M.J. Kean, V.A. Anderson, M.L. Seal**Automated alignment of perioperative MRI scans: a technical note and application in pediatric epilepsy surgery**
Hum. Brain Mapp., 37 (2016), pp. 3530-3543,

A.O. Blenkmann, H.N. Phillips, J.P. Princich, J.B. Rowe, T.A. Bekinschtein, C.H. Muravchik, S. Kocheni**iElectrodes: a comprehensive open-source toolbox for depth and subdural grid electrode localization**
Front. Neuroinform., 11 (2017), pp. 1-16, 10.3389/fninf.2017.00014
Google Scholar

M.P. Branco, A. Gaglianese, D.R. Glen, D. Hermes, Z.S. Saad, N. Petridou, N.F. Ramsey **ALICE: a tool for automatic localization of intra-cranial electrodes for clinical and high-density grids**
J. Neurosci. Methods, 301 (2018), pp. 43-51, 10.1016/j.jneumeth.2017.10.022
ArticleDownload PDFView Record in ScopusGoogle Scholar

R.L. Buckner, D. Head, J. Parker, A.F. Fotenos, D. Marcus, J.C. Morris, A.Z. Snyder**A unified approach for morphometric and functional data analysis in young, old, and demented adults using automated atlas-based head size normalization: reliability and validation against manual measurement of total intracranial volume**
Neuroimage, 23 (2004), pp. 724-738, 10.1016/j.neuroimage.2004.06.018
ArticleDownload PDFView Record in ScopusGoogle Scholar

J. Cimbalnik, B. Brinkmann, V. Kremen, P. Jurak, B. Berry, J.Van Gompel, M. Stead, G. Worrell**Physiological and pathological high frequency oscillations in focal epilepsy**
Ann. Clin. Transl. Neurol., 5 (2018), pp. 1062-1076, 10.1002/acn3.618
CrossRefView Record in ScopusGoogle Scholar

S.S. Dalal, E. Edwards, H.E. Kirsch, N.M. Barbaro, R.T. Knight, S.S. Nagarajan**Localization of neurosurgically implanted electrodes via photograph-MRI-radiograph coregistration**
J. Neurosci. Methods, 174 (2008), pp. 106-115, 10.1016/j.jneumeth.2008.06.028

ArticleDownload PDFView Record in ScopusGoogle Scholar

K. Ducis, J. Guan, M. Karsy, R.J. Bollo**Preoperative evaluation and surgical decision-making in pediatric epilepsy surgery**
Transl. Pediatr., 5 (2016), pp. 169-179, 10.21037/tp.2016.06.02
CrossRefView Record in ScopusGoogle Scholar

A.R. Dykstra, A.M. Chan, B.T. Quinn, R. Zepeda, C.J. Keller, J. Cormier, J.R. Madsen, E.N. Eskandar, S.S. Cash**Individualized localization and cortical surface-based registration of intracranial electrodes**
Neuroimage, 59 (2012), pp. 3563-3570, 10.1016/j.neuroimage.2011.11.046
ArticleDownload PDFView Record in ScopusGoogle Scholar

W.J. Elias, K.M. Fu, R.C. Frysinger**Cortical and subcortical brain shift during stereotactic procedures**
J. Neurosurg., 107 (2007), pp. 983-988, 10.3171/JNS-07/11/0983
View Record in ScopusGoogle Scholar

B. Fischl. **FreeSurfer**
Neuroimage (2012), 10.1016/j.neuroimage.2012.01.021
Google Scholar

S.V. Gliske, Z.T. Irwin, C. Chestek, G.L. Hegeman, B. Brinkmann, O. Sagher, H.J.L. Garton, G.A. Worrell, W.C. Stacey**Variability in the location of high frequency oscillations during prolonged intracranial EEG recordings**
Nat. Commun., 9 (2018), 10.1038/s41467-018-04549-2
Google Scholar

P. Hastreiter, C. Rezk-Salama, G. Soza, M. Bauer, G. Greiner, R. Fahlbusch, O. Ganslandt, C. Nimsky**Strategies for brain shift evaluation**
Med. Image Anal., 8 (2004), pp. 447-464, 10.1016/j.media.2004.02.001
ArticleDownload PDFView Record in ScopusGoogle Scholar

D. Hermes, K.J. Miller, H. Jan, M.J. Vansteensel, N.F. Ramsey**Automated electrocorticographic electrode localization on individually rendered brain surfaces**
J. Neurosci. Methods, 185 (2010), pp. 293-298, 10.1016/j.jneumeth.2009.10.005
ArticleDownload PDFView Record in ScopusGoogle Scholar



D.L.G. Hill, C.R. Maurer, R.J. Maciunas, J.A. Barwise, J.M. Fitzpatrick, M.Y. Wang**Measurement of intraoperative brain surface deformation under a craniotomy**
Neurosurgery, 43 (1998), pp. 514-526, 10.1097/00006123-199809000-00066
View Record in ScopusGoogle Scholar

W.A. Hinds, A. Misra, M.R. Sperling, A. Sharan, J.I. Tracy, K.A. Moxon**Enhanced co-registration methods to improve intracranial electrode contact localization**
Neuroimage Clin., 20 (2018), pp. 398-406, 10.1016/j.nicl.2018.07.026

ArticleDownload PDFView Record in ScopusGoogle Scholar

M.E. Ivan, J. Yarlagadda, A.P. Saxena, A.J. Martin, P.A. Starr, W.K. Sootsman, P.S. Larson**Brain shift during bur hole-based procedures using interventional MRI: clinical article**
J. Neurosurg., 121 (2014), pp. 149-160, 10.3171/2014.3.JNS121312
View Record in ScopusGoogle Scholar

J. Jacobs, J.Y. Wu, P. Perucca, R. Zelmann, M. Mader, F. Dubeau, G.W. Mathern, A. Schulze-Bonhage, J. Gotman**Removing high-frequency oscillations: a prospective multicenter study on seizure outcome**
Neurology, 91 (2018), pp. e1040-e1052, 10.1212/WNL.0000000000006158
CrossRefView Record in ScopusGoogle Scholar

P.S. LaViolette, S.D. Rand, B.M. Ellingson, M. Raghavan, S.M. Lew, K.M. Schmainda, W. Mueller**3D visualization of subdural electrode shift as measured at craniotomy reopening**
Epilepsy Res., 94 (2011), pp. 102-109, 10.1016/j.eplepsyres.2011.01.011
ArticleDownload PDFView Record in ScopusGoogle Scholar

5

M.M.J. Letteboer, P.W.A. Willems, M.A. Viergever, W.J. Niessen**Brain shift estimation in image-guided neurosurgery using 3-D ultrasound**
IEEE Trans. Biomed. Eng., 52 (2005), pp. 268-276, 10.1109/TBME.2004.840186
View Record in ScopusGoogle Scholar

1

A. Nabavi, P. McL
Black, D.T. Gering, C.F. Westin, V. Mehta, R.S. Pergolizzi, M. Ferrant, S.K. Warfield, N. Hata, R.B. Schwartz, W.M. Wells, R. Kikinis, F.A. Jolesz**Serial intraoperative magnetic resonance imaging of brain shift**
Neurosurgery, 48 (2001), pp. 787-798, 10.1227/00006123-200104000-00019
CrossRefView Record in ScopusGoogle Scholar

0

C. Nimsky, O. Ganslandt, S. Cerny, P. Hastreiter, G. Greiner, R. Fahlbusch**Quantification of, visualization of, and compensation for brain shift using intraoperative magnetic resonance imaging**
Neurosurgery, 47 (2000), pp. 1070-1079, 10.1097/00006123-200011000-00008
discussion 1079-1080
View Record in ScopusGoogle Scholar

7

W. Penny, K. Friston, J. Ashburner, S. Kiebel, T. Nichols**Statistical parametric mapping: the analysis of functional brain images**
Statistical Parametric Mapping: The Analysis of Functional Brain Images (1st ed), Elsevier, San Diego, CA (2007), 10.1016/B978-0-12-372560-8.X5000-1
Google Scholar

8

D.W. Roberts, A. Hartov, F.E. Kennedy, M.I. Miga, K.D. Paulsen, R.J. Maciunas, P.J. Kelly, R.A.E. Bakay, G.H. Barnett**Intraoperative brain shift and deformation: a quantitative analysis of cortical displacement in 28 cases**
Neurosurgery, 43 (1998), pp. 758-760, 10.1097/00006123-199810000-00010
View Record in ScopusGoogle Scholar

8

M. Schaer, M. Bach Cuadra, L. Tamarit, F. Lazeyras, S. Eliez, J.P. Thiran**A Surface-based approach to quantify local cortical gyrification**
IEEE Trans. Med. Imaging, 27 (2008), pp. 161-170, 10.1109/TMI.2007.903576
View Record in ScopusGoogle Scholar

3

K.A. Sillay, L.M. Kumbier, C. Ross, M. Brady, A. Alexander, A. Gupta, N. Adluru, G.S. Miranpuri, J.C. Williams**Perioperative brain shift and deep brain stimulating electrode deformation analysis: implications for rigid and non-rigid devices**
Ann. Biomed. Eng., 41 (2013), pp. 293-304, 10.1007/s10439-012-0650-0
CrossRefView Record in ScopusGoogle Scholar

O. Škrinjar, A. Nabavi, J. Duncan**Model-driven brain shift compensation**
Med. Image Anal., 6 (2002), pp. 361-373, 10.1016/S1361-8415(02)00062-2
ArticleDownload PDFView Record in ScopusGoogle Scholar

8

A. Stolk, S. Griffin, R. Van Der
Meij, C. Dewar, I. Saez, J.J. Lin, G. Piantoni, J.M. Schoffelen, R.T. Knight, R. Oostenveld**Integrated analysis of anatomical and electrophysiological human intracranial data**
Nat. Protoc., 13 (2018), pp. 1699-1723, 10.1038/s41596-018-0009-6
CrossRefView Record in ScopusGoogle Scholar

V. Taimouri, A. Akhondi-Asl, X. Tomas-Fernandez, J.M. Peters, S.P. Prabhu, A. Poduri, M. Takeoka, T. Loddenkemper, A.M.R. Bergin, C. Harini, J.R. Madsen, S.K. Warfield, A.A. Xavier, T.J.M. Peters, S.P. Prabhu, A. Poduri, M. Takeoka, T. Loddenkemper, A. Marie, R.B. Chellamani, H. Joseph, R.M. Simon, A. Akhondi-Asl, X. Tomas-Fernandez, J.M. Peters, S.P. Prabhu, A. Poduri, M. Takeoka, T. Loddenkemper, A.M.R. Bergin, C. Harini, J.R. Madsen, S.K. Warfield, A.A. Xavier, T.J.M. Peters, S.P. Prabhu, A. Poduri, M. Takeoka, T. Loddenkemper, A. Marie, R.B. Chellamani, H. Joseph, R.M. Simon, A. Akhondi-Asl, X. Tomas-Fernandez, J.M. Peters, S.P. Prabhu, A. Poduri, M. Takeoka, T. Loddenkemper, A.M.R. Bergin, C. Harini, J.R. Madsen, S.K. Warfield**Electrode localization for planning surgical resection of the epileptogenic zone in pediatric epilepsy**
Int. J. Comput. Assist. Radiol. Surg., 9 (2014), pp. 91-105, 10.1007/s11548-013-0915-6
CrossRefView Record in ScopusGoogle Scholar

B.D. Van Rooijen, W.H. Backes, O.E.M.G. Schijns, A. Colon, P.A.M. Hofman**Brain imaging in chronic epilepsy patients after depth electrode (stereoelectroencephalography) implantation: magnetic resonance imaging or computed tomography?**
Neurosurgery, 73 (2013), pp. 543-549, 10.1227/01.neu.0000431478.79536.68

CrossRefView Record in ScopusGoogle Scholar

C. Wu, W.J. Jermakowicz, S. Chakravorti, I. Cajigas, A.D. Sharan, J.R. Jagid, C.M. Mati as, M.R. Sperling, R. Buckley, A. Ko, J.G. Ojemann, J.W. Miller, B. Youngerman, S.A. Sheth, G.M. McKhann, A.W. Laxton, D.E. Couture, G.S. Popli, A. Smith, A.D. Mehta, A .L. Ho, C.H. Halpern, D.J. Englot, J.S. Neimat, P.E. Konrad, E. Neal, F.L. Vale, K.L. Hol loway, E.L. Air, J. Schwalb, B.M. Dawant, P.F. D'Haese**Effects of surgical targeting in laser interstitial thermal therapy for mesial temporal lobe epilepsy: a multicenter study of 234 patients**
Epilepsia, 60 (2019), pp. 1171-1183, 10.1111/epi.15565
View Record in ScopusGoogle Scholar

2

A.I. Yang, X. Wang, W.K. Doyle, E. Halgren, C. Carlson, T.L. Belcher, S.S. Cash, O. De vinsky, T. Thesen**Localization of dense intracranial electrode arrays using magnetic resonance imaging**
Neuroimage, 63 (2012), pp. 157-165, 10.1016/j.neuroimage.2012.06.039
ArticleDownload PDFView Record in ScopusGoogle Scholar

7

J.Y. Yang, R. Beare, M.L. Seal, A.S. Harvey, V.A. Anderson, W.J. Maixner**A systematic evaluation of intraoperative white matter tract shift in pediatric epilepsy surgery using high-field MRI and probabilistic high angular resolution diffusion imaging tractography**
J. Neurosurg. Pediatr., 19 (2017), pp. 1-14, 10.3171/2016.11.PEDS16312
CrossRefView Record in ScopusGoogle Scholar